

UC Irvine

UC Irvine Previously Published Works

Title

Heterogeneous OH Oxidation, Shielding Effects, and Implications for the Atmospheric Fate of Terbutylazine and Other Pesticides

Permalink

<https://escholarship.org/uc/item/75j5k9ff>

Journal

Environmental Science and Technology, 51(23)

ISSN

0013-936X

Authors

Socorro, Joanna
Lakey, Pascale SJ
Han, Lei
et al.

Publication Date

2017-12-05

DOI

10.1021/acs.est.7b04307

Peer reviewed

Heterogeneous OH Oxidation, Shielding Effects, and Implications for the Atmospheric Fate of Terbutylazine and Other Pesticides

Joanna Socorro,[†] Pascale S. J. Lakey,^{*,†,‡} Lei Han,[§] Thomas Berkemeier,^{||} Gerhard Lammel,^{†,⊥} Cornelius Zetzsch,^{†,§} Ulrich Pöschl,^{*,†} and Manabu Shiraiwa^{*,†} 

[†]Multiphase Chemistry Department, Max Planck Institute for Chemistry, 55128 Mainz, Germany

[‡]Department of Chemistry, University of California, Irvine, California 92617, United States

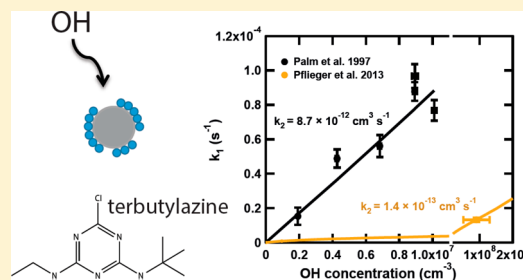
[§]Forschungsstelle für Atmosphärische Chemie, University of Bayreuth, 95440 Bayreuth, Germany

^{||}School of Chemical & Biomolecular Engineering, Georgia Institute of Technology, Atlanta, Georgia 30332, United States

[⊥]Research Centre for Toxic Compounds in the Environment, Masaryk University, 62500 Brno, Czech Republic

Supporting Information

ABSTRACT: Terbutylazine (TBA) is a widely used herbicide, and its heterogeneous reaction with OH radicals is important for assessing its potential to undergo atmospheric long-range transport and to affect the environment and public health. The apparent reaction rate coefficients obtained in different experimental investigations, however, vary by orders of magnitude depending on the applied experimental techniques and conditions. In this study, we used a kinetic multilayer model of aerosol chemistry with reversible surface adsorption and bulk diffusion (KM-SUB) in combination with a Monte Carlo genetic algorithm to simulate the measured decay rates of TBA. Two experimental data sets available from different studies can be described with a consistent set of kinetic parameters resolving the interplay of chemical reaction, mass transport, and shielding effects. Our study suggests that mass transport and shielding effects can substantially extend the atmospheric lifetime of reactive pesticides from a few days to weeks, with strong implications for long-range transport and potential health effects of these substances.



INTRODUCTION

Chemical transformation of pesticides in the atmosphere due to photolysis and by reactions with oxidants such as hydroxyl radicals, nitrate radicals, and ozone impacts their atmospheric lifetimes and their effects on the environment and public health.^{1–4} OH radicals play a critical role in oxidizing organic compounds in the atmosphere, and gas-phase reactions of pesticides with OH radicals are relatively well understood.⁵ Heterogeneous and multiphase reactions of OH are also important pathways for degrading organic compounds in the atmosphere, but an experimental investigation of OH uptake and reactions is a challenging task.^{6–10} Consequently, heterogeneous loss of herbicides and other pesticides by OH radicals are so far poorly characterized and quantified.^{11,12} A lack of understanding of their reactivity in the particulate phase causes high uncertainty in the evaluation of their fate in the atmosphere.

Terbutylazine (TBA) is a semivolatile herbicide, which is used in over 45 countries to prevent and control the growth of grasses, mosses, and weeds in agriculture, forestry, gardens, and other outdoor environments. TBA can be emitted in the atmosphere by different processes such as spray drift, volatilization, wind erosion, and dispersion. TBA has a low vapor pressure (0.15 mPa at 298 K), a high octanol-air partitioning coefficient ($\log K_{oa} = 9.03$ ¹³), and has been measured at high concentrations (from 23 to 118 pg m⁻³)

mostly on coarse particles near application areas,^{14,15} and also far from sources such as over the North Sea.¹⁶ TBA is known to induce high long-term risks for mammals, aquatic organisms, nontarget plants, and earthworms¹⁷ and can have genotoxic effects (DNA damage and cancer).^{18,19} Indeed, studies in aquatic organisms found that the toxic mechanism of TBA may include induction of oxidative stress and accumulation of reactive oxygen species in the cell.^{20,21} Oxidation of TBA yields acetyl and desethyl products which have the potential to be toxic as well.²² It is therefore necessary to understand the lifetime and chemical transformation of TBA in the atmosphere.

The reaction rate constant of TBA with OH in the gas phase was estimated by the Atmospheric Oxidation Program (AOP; USEPA, 2012) as $\sim 9.5 \times 10^{-12} \text{ cm}^3 \text{ s}^{-1}$, leading to a lifetime of about 2.4 days in the gas phase at an OH concentration of $5 \times 10^5 \text{ cm}^{-3}$.²³ The heterogeneous reactivity of TBA with OH radicals has so far been investigated in three different peer-reviewed studies, two studies by Palm et al.,^{22,24} and a study by Pflieger et al.²⁵ Palm et al.²² determined an effective second-order rate coefficient between gas-phase OH radicals and TBA adsorbed on

Received: August 21, 2017

Revised: November 3, 2017

Accepted: November 10, 2017

Published: November 10, 2017

silica particles (Aerosil 200) as $1.1 \times 10^{-11} \text{ cm}^3 \text{ s}^{-1}$. This high value was confirmed by a second study by Palm et al.²⁴ However, Pflieger et al.²⁵ determined a rate coefficient which was 2 orders of magnitude lower. The second-order rate coefficient of TBA with OH radicals determined by these studies are therefore not in agreement, leading to uncertainty in predictions of the atmospheric fate of TBA. Moreover, TBA was used as a reference compound in some studies for the determination of heterogeneous kinetics of pesticides toward OH radicals, and thus uncertainty in the TBA rate constant will also lead to large errors in the rate constants of other pesticides that react with the OH radical.^{26–29} Therefore, it is important to resolve the discrepancies between different experimental studies and to determine kinetic parameters that support a mechanistic understanding and reliable calculation of the lifetime and transport of TBA, as well as other semivolatile pesticides in the atmosphere.

Methods and Data. We used a kinetic multilayer model of aerosol chemistry with reversible surface adsorption and bulk diffusion (KM-SUB)^{30,31} in combination with a Monte Carlo genetic algorithm³² to simulate the TBA decay rates observed in two experimental studies. The model is based on fundamental physical and chemical processes (e.g., adsorption/desorption, bulk diffusion, reaction kinetics, etc.), enabling an in-depth understanding of the importance of the different processes controlling the concentrations of species and extrapolation to ambient conditions for estimating atmospheric fate of TBA.

The study of Palm et al.²² was performed in an aerosol smog chamber, and it was reported that TBA was adsorbed on silica particles (Aerosil 200) at a concentration of less than one monolayer, as shown in Figure 1. In reality, these silica particles

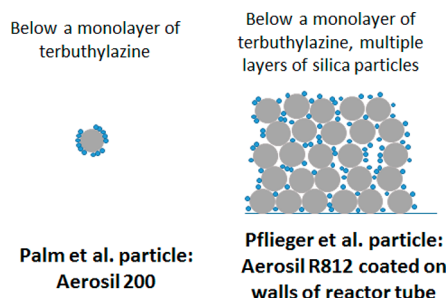


Figure 1. Schematic illustration of the different coating structures of terbuthylazine (TBA) adsorbed on silica particles in the experiments of Palm et al., (1997),²² and Pflieger et al., (2013)²⁵ as treated in the kinetic multilayer model of this study. The gray spheres represent the silica particle, whereas the blue spheres represent the adsorbed TBA molecules. Note that for Pflieger et al. there are actually several hundred layers of silica particles adsorbed to the walls of the reactor tube rather than the five layers shown here.

formed agglomerates as shown in the electron microscope image of such particles in Figure S1 of the Supporting Information, SI. This image shows that the agglomerates are highly porous, indicating that OH radicals can efficiently penetrate these agglomerates by rapid gas-phase diffusion. In the model, we thus assumed single particles for the Palm experiments, and that only a negligible OH radical concentration gradient would be expected across the agglomerate, with both silica particles on the edge and in the center of the agglomerate being exposed to the same concentration of OH radicals. However, if in reality there was a large OH gradient across the agglomerate, then the effective rate coefficient would be underestimated and mass

diffusion limitations would play a role, as will be discussed in further detail in the Results and Discussion section. We have used the data of TBA decay rates with OH radicals generated by photolysis of O₃ or H₂O₂.²² In the experiments of Pflieger et al.,²⁵ R812 silica particles were coated onto the walls of a flow reactor. Pflieger et al.²⁵ reported that the surface coverage of TBA on the surface of the R812 silica particles was below a monolayer (Figure 1).

The kinetic multilayer model of aerosol surface and bulk chemistry (KM-SUB)³¹ was applied to the experimental data of Palm et al.²² and Pflieger et al.²⁵ KM-SUB treats reversible adsorption, surface and bulk reactions, and diffusion in the gas-phase and in the bulk material. For the Palm et al. data the TBA on the particle surface was treated as a submonolayer, and the model did not include processes in the bulk of the particle, as the silica core of the particle is a solid with no possible diffusion. The reaction of OH radicals with the silica surface or with reaction products is assumed to be negligible. However, note that a background was subtracted for the data of Palm et al.²² which corresponds to a rate constant for the loss processes not initialized by OH radicals, such as evaporation of TBA.²² For the Pflieger data, the silica particles and pesticide coating on the flow tube walls were treated as a quasi-homogeneously mixed thin film, with an identical concentration of TBA in each layer of the bulk. Note that in reality the bulk is an agglomerate of silica particles deposited in a flow tube (multilayers of silica particles). The effective bulk TBA concentration was calculated from the amount of TBA deposited on the silica particles and from the volume of the silica particles which was estimated as $\sim 5 \times 10^{17} \text{ cm}^{-3}$. The total thickness of the coating on the walls of the flow reactor, which encompasses both TBA and silica particles, was estimated to be about $1.9 \mu\text{m}$. Kinetic limitations of gas-phase diffusion of OH radicals to the surface of the flow tube are negligible under experimental conditions, as described by Pflieger et al. (2013)²⁵ and thus neglected in the model. Note that only one data point is available in the Pflieger data and fitting to this data is associated with larger uncertainty.

As summarized in Table 1, the kinetic model parameters include the surface accommodation coefficient, desorption lifetime and partitioning coefficient of OH, bulk diffusion coefficients of OH and TBA, and second-order rate coefficients for surface and bulk reactions between OH and TBA. The Monte Carlo Genetic Algorithm (MCGA)³² was applied for simultaneously fitting the kinetic models to the experimental data and determining the unprescribed kinetic parameters listed in Table 1. The MCGA method consists of two steps; a Monte Carlo step and a genetic algorithm step. During the Monte Carlo step the parameters are randomly varied over a range of values and the residue between the model result and the experimental data is determined for each parameter set. During the genetic algorithm step, the best parameter sets are optimized using the processes known from natural evolution of survival, recombination and mutation.³² Based on previous studies, the surface accommodation coefficient and desorption lifetime of OH were fixed at 1 and 10^{-9} s , respectively.^{33–35} The gas-particle partitioning coefficient was set to a value which is within the range of OH Henry's law coefficients that have been reported in the literature ($K_{\text{OH}} = 0.029 \text{ mol cm}^{-3} \text{ atm}^{-1}$).^{36,37} D_{OH} , D_{TBA} , K_{OH} , and $k_{\text{br,OH}}$ were fixed to zero for the Palm et al. data due to the lack of a bulk into which OH radicals could diffuse. D_{TBA} was fixed to zero for the Pflieger et al. experiments, assuming that TBA is adsorbed on the silica particles at a concentration corresponding to less than one monolayer.

Table 1. Kinetic Parameters for the Heterogeneous Oxidation of TBA by OH Radicals Obtained by the Fitting of a Kinetic Multilayer Model (KM-SUB) to Two Different Experimental Data Sets Taken from the Peer-Reviewed Studies of Palm et al.²² and Pflieger et al.^{25a}

symbol	meaning and unit	Palm et al. ²² data	Pflieger et al. ²⁵ data
$\alpha_{s,0,OH}$	surface accommodation coefficient of OH radicals on adsorbate-free substrate	1*	1*
$\tau_{d,OH}$	desorption lifetime of OH radicals (s)	1.0×10^{-9} *	1.0×10^{-9} *
D_{OH}	bulk diffusion coefficient of OH radicals ($\text{cm}^2 \text{s}^{-1}$)	0*	3.1×10^{-7}
D_{TBA}	bulk diffusion coefficient of TBA ($\text{cm}^2 \text{s}^{-1}$)	0*	0*
K_{OH}	gas-particle partitioning coefficient of OH radicals ($\text{mol cm}^{-3} \text{atm}^{-1}$)	0*	0.029*
$k_{slr,OH}$	second-order rate coefficient for surface layer reaction of TBA with OH radicals ($\text{cm}^2 \text{s}^{-1}$)	6.7×10^{-7}	6.7×10^{-7}
$k_{br,OH}$	second-order rate coefficient for bulk reactions of OH radicals ($\text{cm}^3 \text{s}^{-1}$)	0*	1×10^{-14}

^aPrescribed parameter values are marked with an asterisk (*). The value of D_{OH} for the Pflieger et al. data should be considered a lower limit and could change if OH radicals react with methyl groups on the silica particles (see text).

Sensitivity studies were conducted by varying all kinetic parameters as detailed in Table S1. Some of the parameters were found to be codependent or nonorthogonal with other parameters (i.e., a change in one parameter could lead to the same model output if another parameter was also changed),³⁸ and thus the values cannot be determined with certainty, as discussed below. The value of the bulk rate coefficient, $k_{br,OH}$ was determined to be insensitive when modeling the Pflieger et al. experiments and was assumed to a value which is consistent with the high reactivity of OH radicals ($k_{br,OH} = 1 \times 10^{-14} \text{ cm}^3 \text{ s}^{-1}$).³⁴ It should also be noted that reactions of OH with the desethyl and acetyl products²² were not treated in the model as calculations performed using the AOP model (USEPA, 2012) suggested these to be relatively slow compared to the reaction of OH with TBA. The acetyl and desethyl products have a similar structure and molecular weight to TBA and were therefore assumed to be nonvolatile and to have a negligible impact on the bulk viscosity in accordance with the conclusions of a recent study.³⁹ Furthermore, experimental measurements of the evolution of the products over time would have been required to implement a more complex mechanism in the model. The addition of a more complex mechanism in the model could have caused the parameters in Table 1 to slightly change for the Pflieger data, as more species would have reduced the bulk concentration of OH.

RESULTS AND DISCUSSION

Figure 2 shows the first-order decay rate coefficient of TBA (k_1) as a function of gas-phase OH concentrations for the two data sets taken from Palm et al.²² and Pflieger et al.²⁵ The two data sets can be described by a simple second-order rate equation. The different slopes, however, correspond to apparent second-order rate coefficients that deviate by more than 1 order of magnitude with calculated values of $1.4 \times 10^{-13} \text{ cm}^3 \text{ s}^{-1}$ and $8.7 \times 10^{-12} \text{ cm}^3 \text{ s}^{-1}$. With the kinetic multilayer model and simulating a mechanism of reversible surface adsorption and bulk diffusion, however, we are able to fit the two data sets and explain the observed experimental results with a consistent set of fundamental kinetic parameters as shown in Table 1. The consistent model results and kinetic parameters obtained for the different experimental studies and conditions suggest that the deviating apparent second-order rate coefficients are due to the interplay of mass transport and chemical reaction at the surface and in the bulk of the investigated particles. Rate-limiting effects of diffusion lead to an effective shielding of TBA molecules in the bulk. These rate-limiting effects of diffusion can explain the strong deviations of the apparent rate coefficients for Palm et al.²² to Pflieger et al.²⁵

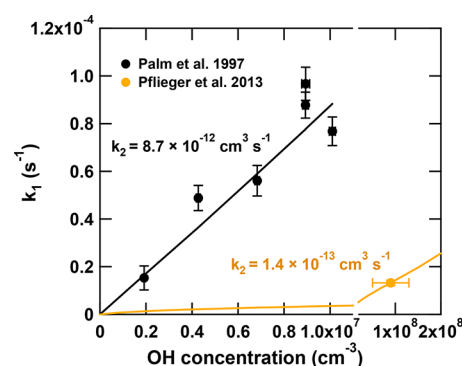


Figure 2. Experimentally observed first-order decay rate coefficients of TBA (k_1) as a function of gas-phase OH concentrations taken from the experimental studies of Palm et al.²² (black circles) and Pflieger et al.²⁵ (yellow circles). The lines represent kinetic multilayer model results obtained with a consistent set of fundamental kinetic parameters (Table 1). The different slopes correspond to different apparent second order rate coefficients (k_2) that are due to the interplay of mass transport limitations and shielding effects in a wall surface coating, which is thicker than one monolayer (Pflieger et al.).

In the Palm study, the TBA surface coverage on the investigated aerosol particles was less than a monolayer, which means that all molecules are directly accessible to adsorbing OH radicals and leads to a high decay rate controlled by the surface adsorption and reaction rate coefficients. However, in the Pflieger study, where the OH radicals need to diffuse through a flow tube wall coating of TBA on tightly packed silica particles, strong shielding effects were observed. OH radicals would first react with TBA adsorbed onto the higher layers of the silica particles, thereby reducing the OH concentration in the lower layers and leading to a decrease in the loss rate of TBA in these layers.

The mechanism, leading to the different apparent rate coefficients between gas-phase OH radicals and particulate-phase TBA, was further explored by sensitivity tests as summarized in Table S1. These studies showed that for the Palm et al. data, the surface accommodation coefficient ($\alpha_{s,0,OH}$), desorption lifetime ($\tau_{d,OH}$), and the second-order rate coefficient for the surface layer reaction ($k_{slr,OH}$) are sensitive, suggesting that the limiting process for the degradation of TBA was the chemical reaction at the surface.⁴⁰ For the Pflieger data, $\tau_{d,OH}$ and $k_{slr,OH}$ are insensitive and $\alpha_{s,0,OH}$ is also insensitive when the value is above 0.05. This insensitivity for parameters describing surface processes confirms that the reaction of TBA is dominated by bulk processes, as also confirmed by the high sensitivity of D_{OH} and K_{OH} . While silica particles used in the Palm study are likely to be

inert to OH, Aerosil R812 particles used in the Pflieger study have methyl groups on the surface that may be reactive toward OH.^{41,42} Sensitivity tests showed that if another reactive species was added into the model at the same concentrations and reactivity as TBA, the Pflieger data point could be reproduced by increasing the bulk diffusion coefficient of OH by a factor of 2. This uncertainty is also reported in Table 1 but does not affect the main conclusions of our work.

Sensitivity studies for the Palm data show that $\tau_{d,OH}$ and $k_{slr,OH}$ are mutually interdependent and exhibit a tight inverse correlation as shown in Figure 3. This is in agreement with the

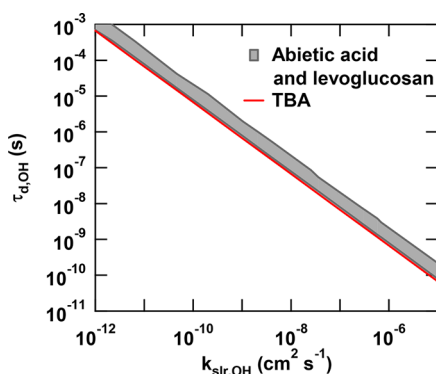


Figure 3. Correlation between desorption lifetime of OH radicals ($\tau_{d,OH}$) and second-order rate coefficient for surface reaction of TBA with OH radicals ($k_{slr,OH}$) for terbuthylazine from Palm²² data (red line). The gray corridor shows corresponding correlation for OH uptake by levoglucosan and abietic acid from Arangio et al. (2015).³⁴

modeling results of Arangio et al.³⁴ for OH uptake by levoglucosan and abietic acid with a very similar slope. Different combinations of $\tau_{d,OH}$ and $k_{slr,OH}$, which span 7 orders of magnitude, can be used to reproduce the experimental data. Molecular dynamic simulations suggest that $\tau_{d,OH}$ for physisorbed OH radicals should be on the order of nanoseconds.³³ For $\tau_{d,OH} \approx 1$ ns we obtain $k_{slr,OH} \approx 7 \times 10^{-7} \text{ cm}^2 \text{ s}^{-1}$, as listed in Table 1. For the Pflieger et al. data, the relationship between $\tau_{d,OH}$ and $k_{slr,OH}$ was more complex due to the model outputs being sensitive to the bulk processes.

The uptake coefficient of OH (γ_{OH}) after a reaction time of one second was modeled to be 0.07 and 0.003 for the Palm et al. and Pflieger et al. data, respectively. γ_{OH} was lower for Pflieger et al.²⁵ due to the lower TBA concentrations on the surface and in the bulk, leading to less reactive loss of OH in the bulk. For the two data sets, values of γ_{OH} are predicted to decrease over time, as the degradation of TBA adsorbed on the surface and in the bulk decreases leading to less reaction with OH radicals.

Figure 4 shows the modeled chemical half-life of TBA in the particle phase as a function of different numbers of TBA layers for atmospherically relevant gas-phase OH concentrations in the range of $10^5 - 2 \times 10^7 \text{ cm}^{-3}$.^{43,44} TBA particle mixing ratios up to $2 \mu\text{g} (\text{g PM})^{-1}$ in coarse and up to $0.3 \mu\text{g} (\text{g PM})^{-1}$ in submicrometer particles have been reported off application areas,⁴⁵ which corresponds to less than 1, but up to ~ 0.1 monolayer on the particle surface. For a single or less than monolayer of TBA and at a typical atmospheric OH concentration of $1 \times 10^6 \text{ cm}^{-3}$, the chemical half-life of TBA is predicted to be approximately 1 day.

The observations of TBA mixing ratios close to sources were about a factor of ~ 50 higher than those off application areas.¹⁵ Moreover, El Masri et al.⁴⁶ have previously shown that although

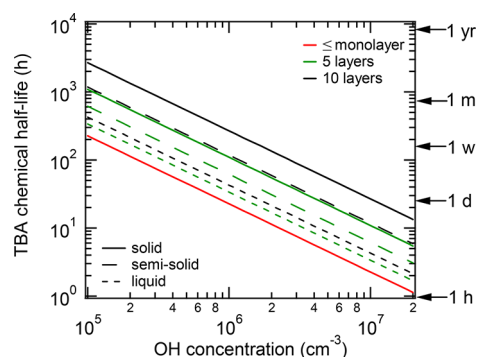


Figure 4. Predicted TBA chemical half-life in the particle phase as a function of surface coating thickness (red: monolayer, green: 5 layers, black: 10 layers) for atmospherically relevant OH concentrations at 25 °C. TBA molecules are assumed to be embedded in amorphous solid ($D_{OH} = 1 \times 10^{-9} \text{ cm}^2 \text{ s}^{-1}$, $D_{TBA} = 1 \times 10^{-18} \text{ cm}^2 \text{ s}^{-1}$), semisolid ($D_{OH} = 1 \times 10^{-7} \text{ cm}^2 \text{ s}^{-1}$, $D_{TBA} = 1 \times 10^{-15} \text{ cm}^2 \text{ s}^{-1}$), and liquid ($D_{OH} = 1 \times 10^{-5} \text{ cm}^2 \text{ s}^{-1}$, $D_{TBA} = 1 \times 10^{-7} \text{ cm}^2 \text{ s}^{-1}$) phase states.

the concentration of the pesticide chlorpyrifos ethyl should also be below one monolayer on atmospheric particles, it can form “heaps” on sand particles thereby extending its lifetime in the atmosphere. Gas-particle partitioning of pesticides including TBA is well predictable assuming absorptive partitioning into octanol.^{45,47} Therefore, particulate phase pesticides are most likely components of organic phases, which can be liquid or amorphous (semi)solid depending on relative humidity and temperature.^{48,49} To assess potential effects of multilayer coatings or an embedding of TBA in an organic phase, estimates of the chemical half-life were also calculated for coating thicknesses of 5 layers (green lines) and 10 layers (red lines) assuming different phase states and characteristic bulk diffusion coefficients:³⁶ amorphous solid ($D_{OH} = 1 \times 10^{-9} \text{ cm}^2 \text{ s}^{-1}$, $D_{TBA} = 1 \times 10^{-18} \text{ cm}^2 \text{ s}^{-1}$), semisolid ($D_{OH} = 1 \times 10^{-7} \text{ cm}^2 \text{ s}^{-1}$, $D_{TBA} = 1 \times 10^{-15} \text{ cm}^2 \text{ s}^{-1}$), and liquid ($D_{OH} = 1 \times 10^{-5} \text{ cm}^2 \text{ s}^{-1}$, $D_{TBA} = 1 \times 10^{-7} \text{ cm}^2 \text{ s}^{-1}$).

The lifetime of TBA depends strongly on the number of layers of TBA on particles and the organic phase state. If the coating thickness increases up to 10 molecular layers, then the TBA half-life increases to ~ 40 h, ~ 4 days, and more than 10 days for a liquid, semisolid or amorphous solid organic phase, respectively, due to kinetic limitations by bulk diffusion of OH and TBA molecules. The differences between the liquid, semisolid, and solid phases can be explained by calculating the reacto-diffusive length ($l = (D_{OH}/(k_{br,OH}[TBA]))^{1/2}$), which is the average traveling distance of OH in the bulk before reacting.⁵⁰ l is initially ~ 6 , ~ 0.6 , and ~ 0.06 nm for a liquid, semisolid, and solid bulk, respectively. These values are consistent with recent studies of OH uptake by organic aerosol surfaces, which found that they are in the range of ~ 1 – 10 nm depending on the phase state.^{9,51,52} These values of l indicate that the reaction will occur close to the surface for an amorphous solid or semisolid phase, but can occur throughout the bulk for a liquid phase, thereby decreasing the chemical half-life.

Our results suggest that mass transport limitations can be important for the atmospheric lifetime and, hence, long-range transport potential of semivolatile organics of similar reactivity, molecular size, and polarity to TBA. Carbamates, thiophosphoric acid esters, phenols, and anilines are substances which usually have a similar molecular size and polarity as TBA and are prominent among currently used pesticides.⁵³ The lifetime of particulate phase pesticides will depend on the atmospheric

relative humidity, which can lead to a change in the phase of these mixtures, the thickness of these layers, as well as the reactivity of the pesticide and the other organic species. Chemical aging of organic compounds can be limited by bulk diffusion if pesticides are embedded in an organic phase, as also recently demonstrated by a number of studies.^{8,9,36,39,54–59} Moreover, the actual morphology, mixing, and phase state may depend on the type of particle that the pesticide is adsorbing to. Further experimental and field studies are required to fully understand and quantify the morphology, mixing and phase state of pesticides in atmospheric aerosols, and how much shielding effects actually extend the lifetime of pesticides under atmospheric conditions.

■ ASSOCIATED CONTENT

Supporting Information

The Supporting Information is available free of charge on the ACS Publications website at DOI: 10.1021/acs.est.7b04307.

Image of Aerosil particles typical of the Palm et al. experiments; sensitivity analysis for the model simulations; and additional references (PDF)

■ AUTHOR INFORMATION

Corresponding Authors

*E-mail: plakey@uci.edu (P.S.J.L.).

*E-mail: u.poschl@mpic.de (U.P.).

*E-mail: m.shiraiwa@uci.edu (M.S.).

ORCID

Manabu Shiraiwa: 0000-0003-2532-5373

Notes

The authors declare no competing financial interest.

■ ACKNOWLEDGMENTS

This work was funded by the Umweltbundesamt, by the EU (infrastructure EUROCHAMP), the University of Bayreuth, the DFG research unit (HA LOPROC (792)), the Max Planck Society, the School of Physical Sciences at UC Irvine and the National Science Foundation (AGS, No. 1654104).

■ REFERENCES

- (1) Atkinson, R.; Arey, J. Gas-phase tropospheric chemistry of biogenic volatile organic compounds: a review. *Atmos. Environ.* **2003**, *37*, 197–219.
- (2) Finlayson-Pitts, B. J.; Pitts, J. N. Tropospheric air pollution: ozone, airborne toxics, polycyclic aromatic hydrocarbons, and particles. *Science* **1997**, *276*, 1045–1051.
- (3) Chapleski, R. C.; Zhang, Y.; Troya, D.; Morris, J. R. Heterogeneous chemistry and reaction dynamics of the atmospheric oxidants, O₃, NO₃, and OH, on organic surfaces. *Chem. Soc. Rev.* **2016**, *45*, 3731–3746.
- (4) Hebert, V.; Miller, G. Understanding the tropospheric transport and fate of agricultural pesticides. In *Reviews of Environmental Contamination and Toxicology*; Springer: New York, 2004; pp 1–36.
- (5) Finlayson-Pitts, B. J.; Pitts, J. N., Jr *Chemistry of the Upper and Lower Atmosphere*; In Academic Press: San Diego, 2000; pp 871–942.
- (6) Bertram, A. K.; Ivanov, A. V.; Hunter, M.; Molina, L. T.; Molina, M. J. The reaction probability of OH on organic surfaces of tropospheric interest. *J. Phys. Chem. A* **2001**, *105*, 9415–9421.
- (7) McNeill, V.; Yatavelli, R.; Thornton, J.; Stipe, C.; Landgrebe, O. Heterogeneous OH oxidation of palmitic acid in single component and internally mixed aerosol particles: vaporization and the role of particle phase. *Atmos. Chem. Phys.* **2008**, *8*, 5465–5476.
- (8) Slade, J. H.; Knopf, D. A. Multiphase OH oxidation kinetics of organic aerosol: The role of particle phase state and relative humidity. *Geophys. Res. Lett.* **2014**, *41*, 5297–5306.
- (9) Davies, J. F.; Wilson, K. R. Nanoscale interfacial gradients formed by the reactive uptake of OH radicals onto viscous aerosol surfaces. *Chem. Sci.* **2015**, *6*, 7020–7027.
- (10) Slade, J. H.; Knopf, D. A. Heterogeneous OH oxidation of biomass burning organic aerosol surrogate compounds: assessment of volatilisation products and the role of OH concentration on the reactive uptake kinetics. *Phys. Chem. Chem. Phys.* **2013**, *15*, 5898–5915.
- (11) Socorro, J.; Durand, A.; Temime-Roussel, B.; Gligorovski, S.; Wortham, H.; Quivet, E. The persistence of pesticides in atmospheric particulate phase: An emerging air quality issue. *Sci. Rep.* **2016**, *6*, 33456–33462.
- (12) Segal-Rosenheimer, M.; Linker, R.; Dubowski, Y. Heterogeneous oxidation of the insecticide cypermethrin as thin film and airborne particles by hydroxyl radicals and ozone. *Phys. Chem. Chem. Phys.* **2011**, *13*, 506–517.
- (13) Yusà, V.; Coscollà, C.; Millet, M. New screening approach for risk assessment of pesticides in ambient air. *Atmos. Environ.* **2014**, *96*, 322–330.
- (14) Coscollà, C.; León, N.; Pastor, A.; Yusà, V. Combined target and post-run target strategy for a comprehensive analysis of pesticides in ambient air using liquid chromatography-Orbitrap high resolution mass spectrometry. *J. Chromatogr. A* **2014**, *1368*, 132–142.
- (15) Coscollà, C.; Muñoz, A.; Borrás, E.; Vera, T.; Ródenas, M.; Yusà, V. Particle size distributions of currently used pesticides in ambient air of an agricultural Mediterranean area. *Atmos. Environ.* **2014**, *95*, 29–35.
- (16) Mai, C.; Theobald, N.; Lammel, G.; Hühnerfuss, H. Spatial, seasonal and vertical distributions of currently-used pesticides in the marine boundary layer of the North Sea. *Atmos. Environ.* **2013**, *75*, 92–102.
- (17) European Food Safety, A. Conclusion on the peer review of the pesticide risk assessment of the active substance terbuthylazine. *EFSA J.* **2011**, *9*, 1969.
- (18) Mladinic, M.; Zeljezic, D.; Shaposhnikov, S. A.; Collins, A. R. The use of FISH-comet to detect c-Myc and TP 53 damage in extended-term lymphocyte cultures treated with terbuthylazine and carbofuran. *Toxicol. Lett.* **2012**, *211*, 62–69.
- (19) Lovaković, B. T.; Pizent, A.; Kašuba, V.; Kopjar, N.; Micek, V.; Mendaš, G.; Dvorščak, M.; Mikolić, A.; Milić, M.; Žunec, S. Effects of sub-chronic exposure to terbuthylazine on DNA damage, oxidative stress and parent compound/metabolite levels in adult male rats. *Food Chem. Toxicol.* **2017**, *108*, 93–103.
- (20) Plhalova, L.; Stepanova, S.; Blahova, J.; Praskova, E.; Hostovsky, M.; Skoric, M.; Zelnickova, L.; Svobodova, Z.; Bedanova, I. The effects of subchronic exposure to terbuthylazine on zebrafish. *Neuroendocrinol. Lett.* **2012**, *33*, 113–119.
- (21) Velisek, J.; Koutnik, D.; Zuskova, E.; Stara, A. Effects of the terbuthylazine metabolite terbuthylazine-desethyl on common carp embryos and larvae. *Sci. Total Environ.* **2016**, *539*, 214–220.
- (22) Palm, W.-U.; Elend, M.; Krueger, H.-U.; Zetzsch, C. OH radical reactivity of airborne terbuthylazine adsorbed on inert aerosol. *Environ. Sci. Technol.* **1997**, *31*, 3389–3396.
- (23) Meylan, W. M.; Howard, P. H. Computer estimation of the atmospheric gas-phase reaction rate of organic compounds with hydroxyl radicals and ozone. *Chemosphere* **1993**, *26*, 2293–2299.
- (24) Palm, W.-U.; Millet, M.; Zetzsch, C. OH radical reactivity of pesticides adsorbed on aerosol materials: first results of experiments with filter samples. *Ecotoxicol. Environ. Saf.* **1998**, *41*, 36–43.
- (25) Pflieger, M.; Monod, A.; Wortham, H. Heterogeneous oxidation of terbuthylazine by “dark” OH radicals under simulated atmospheric conditions in a flow tube. *Environ. Sci. Technol.* **2013**, *47*, 6239–6246.
- (26) Al Rashidi, M.; Chakir, A.; Roth, E. Heterogeneous oxidation of folpet and dimethomorph by OH radicals: A kinetic and mechanistic study. *Atmos. Environ.* **2014**, *82*, 164–171.
- (27) Al Rashidi, M.; El Mouden, O.; Chakir, A.; Roth, E.; Salghi, R. The heterogeneous photo-oxidation of difenoconazole in the atmosphere. *Atmos. Environ.* **2011**, *45*, 5997–6003.
- (28) El Masri, A.; Al Rashidi, M.; Laversin, H.; Chakir, A.; Roth, E. A mechanistic and kinetic study of the heterogeneous degradation of

chlorpyrifos and chlorpyrifos oxon under the influence of atmospheric oxidants: ozone and OH-radicals. *RSC Adv.* **2014**, *4*, 24786–24795.

(29) Bouya, H.; Errami, M.; Chakir, A.; Roth, E. Kinetics of the heterogeneous photo oxidation of the pesticide bupirimate by OH-radicals and ozone under atmospheric conditions. *Chemosphere* **2015**, *134*, 301–306.

(30) Pöschl, U.; Rudich, Y.; Ammann, M. Kinetic model framework for aerosol and cloud surface chemistry and gas-particle interactions - Part 1: General equations, parameters, and terminology. *Atmos. Chem. Phys.* **2007**, *7*, 5989–6023.

(31) Shiraiwa, M.; Pfrang, C.; Pöschl, U. Kinetic multi-layer model of aerosol surface and bulk chemistry (KM-SUB): the influence of interfacial transport and bulk diffusion on the oxidation of oleic acid by ozone. *Atmos. Chem. Phys.* **2010**, *10*, 3673–3691.

(32) Berkemeier, T.; Ammann, M.; Krieger, U. K.; Peter, T.; Spichtinger, P.; Pöschl, U.; Shiraiwa, M.; Huisman, A. J. Technical note: Monte Carlo genetic algorithm (MCGA) for model analysis of multiphase chemical kinetics to determine transport and reaction rate coefficients using multiple experimental data sets. *Atmos. Chem. Phys.* **2017**, *17*, 8021–8029.

(33) Vieceli, J.; Roeselova, M.; Potter, N.; Dang, L. X.; Garrett, B. C.; Tobias, D. J. Molecular dynamics simulations of atmospheric oxidants at the air–water interface: solvation and accommodation of OH and O₃. *J. Phys. Chem. B* **2005**, *109*, 15876–15892.

(34) Arangio, A. M.; Slade, J. H.; Berkemeier, T.; Pöschl, U.; Knopf, D. A.; Shiraiwa, M. Multiphase chemical kinetics of OH radical uptake by molecular organic markers of biomass burning aerosols: humidity and temperature dependence, surface reaction, and bulk diffusion. *J. Phys. Chem. A* **2015**, *119*, 4533–4544.

(35) Shiraiwa, M.; Sosedova, Y.; Rouvière, A.; Yang, H.; Zhang, Y.; Abbatt, J. P.; Ammann, M.; Pöschl, U. The role of long-lived reactive oxygen intermediates in the reaction of ozone with aerosol particles. *Nat. Chem.* **2011**, *3*, 291–295.

(36) Shiraiwa, M.; Ammann, M.; Koop, T.; Pöschl, U. Gas uptake and chemical aging of semisolid organic aerosol particles. *Proc. Natl. Acad. Sci. U. S. A.* **2011**, *108*, 11003–11008.

(37) Sander, R. Compilation of Henry's law constants (version 4.0) for water as solvent. *Atmos. Chem. Phys.* **2015**, *15*, 4399–4981.

(38) Berkemeier, T.; Steimer, S. S.; Krieger, U. K.; Peter, T.; Pöschl, U.; Ammann, M.; Shiraiwa, M. Ozone uptake on glassy, semi-solid and liquid organic matter and the role of reactive oxygen intermediates in atmospheric aerosol chemistry. *Phys. Chem. Chem. Phys.* **2016**, *18*, 12662–12674.

(39) Shiraiwa, M.; Li, Y.; Tsimpidi, A. P.; Karydis, V. A.; Berkemeier, T.; Pandis, S. N.; Lelieveld, J.; Koop, T.; Pöschl, U. Global distribution of particle phase state in atmospheric secondary organic aerosols. *Nat. Commun.* **2017**, *8*, 15002.

(40) Berkemeier, T.; Huisman, A. J.; Ammann, M.; Shiraiwa, M.; Koop, T.; Pöschl, U. Kinetic regimes and limiting cases of gas uptake and heterogeneous reactions in atmospheric aerosols and clouds: a general classification scheme. *Atmos. Chem. Phys.* **2013**, *13*, 6663–6686.

(41) Mathias, J.; Wannemacher, G. Basic characteristics and applications of aerosol: 30. The chemistry and physics of the aerosol Surface. *J. Colloid Interface Sci.* **1988**, *125*, 61–68.

(42) Atkinson, R. Kinetics of the gas-phase reactions of a series of organosilicon compounds with hydroxyl and nitrate (NO₃) radicals and ozone at 297.±. 2 K. *Environ. Sci. Technol.* **1991**, *25*, 863–866.

(43) Hobbs, P. V.; Sinha, P.; Yokelson, R. J.; Christian, T. J.; Blake, D. R.; Gao, S.; Kirchstetter, T. W.; Novakov, T.; Pilewskie, P. Evolution of gases and particles from a savanna fire in South Africa. *J. Geophys. Res. - Atmos.* **2003**, *108*, 8485–8505.

(44) Stone, D.; Whalley, L. K.; Heard, D. E. Tropospheric OH and HO₂ radicals: field measurements and model comparisons. *Chem. Soc. Rev.* **2012**, *41*, 6348–6404.

(45) Degrendele, C.; Okonski, K.; Melymuk, L.; Landlová, L.; Kukučka, P.; Audy, O.; Kohoutek, J.; Čupr, P.; Klánová, J. Pesticides in the atmosphere: a comparison of gas-particle partitioning and particle size distribution of legacy and current-use pesticides. *Atmos. Chem. Phys.* **2016**, *16*, 1531–1544.

(46) El Masri, A.; Laversin, H.; Chakir, A.; Roth, E. Influence of the coating level on the heterogeneous ozonolysis kinetics and product yields of chlorpyrifos ethyl adsorbed on sand particles. *Chemosphere* **2016**, *165*, 304–310.

(47) Harner, T.; Bidleman, T. F. Octanol–air partition coefficient for describing particle/gas partitioning of aromatic compounds in urban air. *Environ. Sci. Technol.* **1998**, *32*, 1494–1502.

(48) Koop, T.; Bookhold, J.; Shiraiwa, M.; Pöschl, U. Glass transition and phase state of organic compounds: dependency on molecular properties and implications for secondary organic aerosols in the atmosphere. *Phys. Chem. Chem. Phys.* **2011**, *13*, 19238–19255.

(49) Mikhailov, E.; Vlasenko, S.; Martin, S. T.; Koop, T.; Pöschl, U. Amorphous and crystalline aerosol particles interacting with water vapor: conceptual framework and experimental evidence for restructuring, phase transitions and kinetic limitations. *Atmos. Chem. Phys.* **2009**, *9*, 9491–9522.

(50) Hanson, D. R.; Ravishankara, A.; Solomon, S. Heterogeneous reactions in sulfuric acid aerosols: A framework for model calculations. *J. Geophys. Res.* **1994**, *99*, 3615–3629.

(51) Lee, L.; Wilson, K. The reactive–diffusive length of OH and ozone in model organic aerosols. *J. Phys. Chem. A* **2016**, *120*, 6800–6812.

(52) Houle, F.; Hinsberg, W.; Wilson, K. Oxidation of a model alkane aerosol by OH radical: the emergent nature of reactive uptake. *Phys. Chem. Chem. Phys.* **2015**, *17*, 4412–4423.

(53) Van den Berg, F.; Kubiak, R.; Benjey, W. G.; Majewski, M. S.; Yates, S. R.; Reeves, G. L.; Smelt, J. H.; Van der Linden, A. M. A. Emission of pesticides into the air. In *Fate of Pesticides in the Atmosphere: Implications for Environmental Risk Assessment*; Springer: New York, 1999; pp 195–218.

(54) Shrivastava, M.; Lou, S.; Zelenyuk, A.; Easter, R. C.; Corley, R. A.; Thrall, B. D.; Rasch, P. J.; Fast, J. D.; Simonich, S. L. M.; Shen, H. Global long-range transport and lung cancer risk from polycyclic aromatic hydrocarbons shielded by coatings of organic aerosol. *Proc. Natl. Acad. Sci. U. S. A.* **2017**, *114*, 1246–1251.

(55) Marshall, F. H.; Miles, R. E.; Song, Y.-C.; Ohm, P. B.; Power, R. M.; Reid, J. P.; Dutcher, C. S. Diffusion and reactivity in ultraviscous aerosol and the correlation with particle viscosity. *Chem. Sci.* **2016**, *7*, 1298–1308.

(56) Zhou, S.; Shiraiwa, M.; McWhinney, R. D.; Pöschl, U.; Abbatt, J. P. Kinetic limitations in gas-particle reactions arising from slow diffusion in secondary organic aerosol. *Faraday Discuss.* **2013**, *165*, 391–406.

(57) Lakey, P. S. J.; Berkemeier, T.; Krapf, M.; Dommen, J.; Steimer, S. S.; Whalley, L. K.; Ingham, T.; Baeza-Romero, M. T.; Pöschl, U.; Shiraiwa, M.; et al. The effect of viscosity and diffusion on the HO₂ uptake by sucrose and secondary organic aerosol particles. *Atmos. Chem. Phys.* **2016**, *16*, 13035–13047.

(58) Steimer, S. S.; Berkemeier, T.; Gilgen, A.; Krieger, U. K.; Peter, T.; Shiraiwa, M.; Ammann, M. Shikimic acid ozonolysis kinetics of the transition from liquid aqueous solution to highly viscous glass. *Phys. Chem. Chem. Phys.* **2015**, *17*, 31101–31109.

(59) Abbatt, J.; Lee, A.; Thornton, J. Quantifying trace gas uptake to tropospheric aerosol: recent advances and remaining challenges. *Chem. Soc. Rev.* **2012**, *41*, 6555–6581.